J Korean Radiol Soc 2000;42:417-424

Olfactory Neuroblastoma: CT and MR Findings[1]

Dong Kyung Lee, M.D., Moon Hee Han, M.D., Kee Hyun Chang, M.D., In-One Kim, M.D., Heung Sik Kang, M.D., Kyung Mo Yeon, M.D.

Purpose : The purpose of our study was to determine the CT and MR imaging features of olfactory neuroblastomas in 15 patients.

Materials and Methods : Fifteen patients with pathologically proven sinonasal olfactory neuroblastomas were included in this study. MRI was performed in 12 cases, and CT in 11, while eight patients underwent both MRI and CT. Features analyzed included the extent of the tumor at the time of presentation, its size and enhancement pattern, erosion or destruction of bony structures adjacent to the tumor, and intratumoral cystic areas. Metastasis to regional lymph nodes of head and neck area was also evaluated.

Results : In all patients, the epicenter of primary tumor was the superior nasal cavity or ethmoid sinuses. In 14 patients, the wall of the nasal cavity including the lamina papyracea was involved, while in 13 there was involvement of the cribriform plate. Intracranial tumor extension was demonstrated in nine patients, and intracranial frank mass formation in four. On MR, eight of 12 masses showed low signal intensity on T1-weighted images, while in 11 cases, T2-weighted images revealed iso- or high intensity. In 11 patients, the tumor showed a prominent enhancement pattern on post-contrast enhanced images, while CT scans showed tumor enhancement in all 12 patients.

Conclusion : Olfactory neuroblastomas generally invade the paranasal sinuses and orbit, and are at Kadish stage B or C at the time at which symptoms suggest the need for a hospital visit. Intracranial tumor extension of the tumor is frequent, but mass formation large enough to be detected radiologically is seen in less than half of all cases.

Index words : Paranasal sinuses, neoplasms
Paranasal sinuses, CT
Paranasal sinuses, MR

Olfactory neuroblastomas, also known as esthesioneuroblastomas, are uncommon tumors originating from the olfactory epithelium of the superior nasal cavity. They may occur at any age although bimodal peaks have been observed in the second and the sixth decades (1). Many studies based on cross-sectional imaging have attempted to differentiate various sinonasal tumors, including olfactory neuroblastomas. Unfortunately, however, these lesions tend to reveal no specific CT or MRI findings, and specific diagnosis is thus very difficult (2, 3). Even pathological differentiation of these tumors may be difficult, though pathologic diagnosis now relies on the histochemical, biochemical and structural demonstration of neural elements as well as electron mi-

[1]Department of Radiology, Seoul National University College of Medicine and the Institute of Radiation Medicine, SNUMRC
Received July 28, 1999 ; Accepted December 27, 1999
*This work was supported by a grant provided by the Clinical Research Fund (01-98-044), Seoul National University Hospital.
Address reprint requests to : Moon Hee Han, M.D., Department of Diagnostic Radiology, Seoul National University Hospital, 28 Yongon-Dong, Chongno-Ku, Seoul, 110-744, Korea.
Tel. 82-2-760-3602 Fax. 82-2-743-6385
E-mail : hanmh@radcom.snu.ac.kr

croscopy (4-6).

It is well known that in olfactory neuroblastoma, intracranial extension of a mass via the olfactory groove, or extension to paranasal sinuses, is frequent (7-9), and for accurate staging and preoperative planning, imaging of these lesions to identify the intracranial and orbital extension of the tumor is therefore essential.

The purpose of this study is to determine the CT and MR imaging features of olfactory neuroblastomas, including the primary extent of the tumors at the time of presentation, in 15 patients.

Materials and Methods

Fifteen patients with pathologically proven sinonasal olfactory neuroblastomas were included in this study. Thirteen were male and two were female, and their age ranged from 14 to 62 (mean, 33.9) years. Five of the patients were in their twenties, three in their teens, two in their sixties, their forties, and their thirties, and one in his fifties. Twelve patients underwent MRI, and eleven CT, while eight underwent both MR and CT; all imaging studies were performed prior to any treatment.

For CT scanning, a CT/T 9800 scanner (General Electric Medical Systems, Milwaukee, WI) or an equivalent third generation CT scanner was used in all eleven patients. Sectional scans with 3-10 mm collimation were obtained at 3-10 mm intervals. Contrast enhanced axial and, when available, coronal images were obtained in all these patients.

For MR imaging, Spin-echo MR images were obtained on various MR imagers; a 1.5 T Signa (General Electric Medical Systems, Milwaukee, WI) (n = 2), a 1.0 T Magnetom Expert (n = 1), a 1.5 T Magnetom (n = 5), a 0.5 T GE-Max (General Electric Medical Systems, Milwaukee, WI) (n = 2), 1.0 T SP (General Electric Medical Systems, Milwaukee, WI) (n = 1), a Toshiba (n = 1) and a 2.0 T Spectro-20000 (Goldstar medical Systems, Seoul, Korea) (n = 1). The imaging parameters were 350-800/14-30(repetition time (TR) msec/echo time (TE) msec) for T1- weighted images, and 2200-6000/ 80-100 (TR/TE) for T2- weighted images. Sectional thickness was 4-5 mm, with an intersection gap of between 4 and 11 mm. Field of view varied from 19-25 cm and acquisition matrix from 192-256×200-256.

Masses were evaluated according to the information provided by pre-contrast T1- and T2-weighted axial images, T1-weighted coronal images, and post-contrast T1-weighted axial images.

In all patients, tumors were mapped according to the CT or MR findings. In the case of patients who underwent both CT and MRI, the extent of the tumor at the time of presentation was evaluated only on the basis of the initial imaging modality performed.

Other imaging features of tumor included size, enhancement pattern, the erosion or destruction of bony structures adjacent to the tumor, and intratumoral cystic areas. In MR evaluation, the signal intensities of the tumor in various imaging sequences were also included. Signal intensities of each tumor at various pulse sequences were compared with those of muscles.

Tumor size is determined on the basis of the greatest tumor diameter, and in order to accurately determine the greatest diameter of a tumor whose longest dimension is parallel to the craniocaudal axis, contiguous images were thus examined. Where CT revealed invasion of the paranasal sinus or orbit, disruption of the continuity of a high-attenuated bony area caused by extension

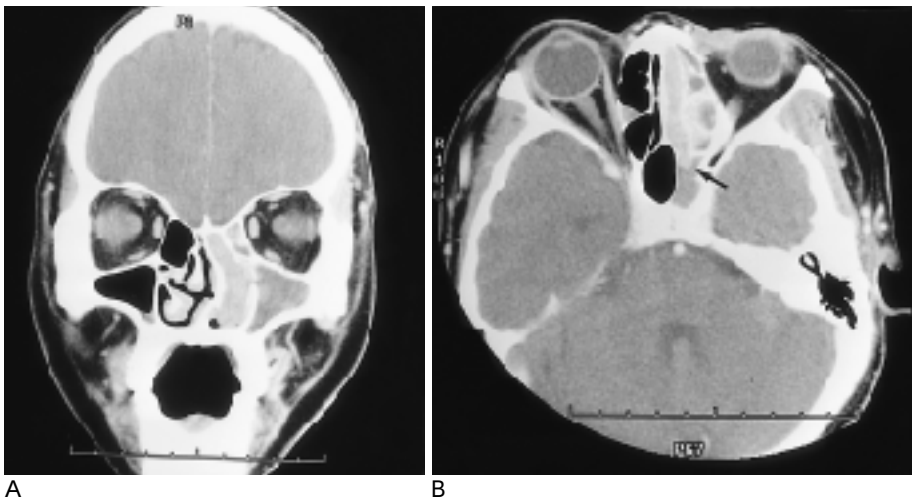

A B

Fig. 1. Sphenoid sinus invasion of olfactory neuroblastoma in a 42-year old man. Contrast enhanced coronal CT image (A) shows well enhancing mass in the left nasal cavity and left ethmoid sinus. The cribriform plate or the left orbital wall does not show any abnormality. Contrast enhanced axial CT image (B) shows focal tumor invasion of the sphenoid sinus (arrow).

of a tumor was considered positive. The MR imaging criterion of adjacent structural invasion by a tumor was discontinuity of the low signal intensity line of bony cortex. Decreased bony thickness by an abutting mass lesion without definite evidence of discontinuity of bony structures was defined as bony erosion. Intratumoral cystic areas were defined as intratumoral areas, with a similar Hounsfield number to that of fluid.

Where images of neck areas were available, metastasis to regional lymph nodes of the head and neck areas was evaluated, and this was possible in 12 patients: CT images were obtained in seven patients, and MR images in eight. Lymph node metastases were considered positive when the respective size of radiologically detected regional lymph nodes was greater than 1cm in long diameter (11).

Results

In all cases, the epicenter of primary tumors was the superior nasal cavity or ethmoid sinuses (Table 1). Bilateral tumor involvement of the ethmoid sinuses was found in eight patients (53%). Evaluation of the initial imaging study showed that in all patients but one (93%), there was involvement of the wall of the nasal cavity including the lamina papyracea. Involvement of the cribriform plate - either erosion or frank destruction - was demonstrated in 13 patients (87%), and in two there was no radiological abnormality of the cribriform plate (Fig. 1). Tumor invasion of the cavernous sinus was demonstrated in one patient (Fig. 2).

In one patient, whose follow-up MRI about one month later showed intracranial tumor involvement, the CT

Table 1. Tumor Mapping, Lymph Node Metastasis, and Tumor Size in 15 Patients with Olfactory Neuroblastoma

Age/Sex	Sphenoid Sinus	Maxillary Siuns	Ethmoid Sinus	Orbital Wall	Cribriform Plate	Intraorbital Iinvasion	Cavernous Sinus	Intracranial Involvement	Intracranial Mass	Neck node Enlargement	Tumor Size (cm)
23/M	-	+	+	+	+	-	-	-	-	-	6
25/M	-	+	+	+	+	-	-	?	-	?	7
36/M	-	+	+	+	+	+	-	+	+	-	4.2
62/M	-	+	+	+	+	-	-	+	+	+	5.7
24/M	+	-	+	+	+	-	+	+	-	+	5
19/F	+	-	+	+	+	-	-	-	-	-	3.5
52/M	-	+	+	+	-	+	-	-	-	+	3.8
42/M	+	+	+	+	+	+	-	+	+	?	8.2
17/M	-	+	+	+	+	+	-	+	-	+	7
62/F	-	-	+	+	+	-	-	-	-	-	4.8
27/M	+	+	+	+	+	+	-	+	+	+	10
24/M	+	+	+	+	+	-	-	+	-	-	5
42/M	+	-	+	-	-	-	-	-	-	-	4.2
13/M	-	-	+	+	+	+	-	+	-	+	5.5
36/M	-	-	+	+	+	+	-	+	+	?	7.2

+: Involved; -: Not Involved; ?: Unable to Evaluate

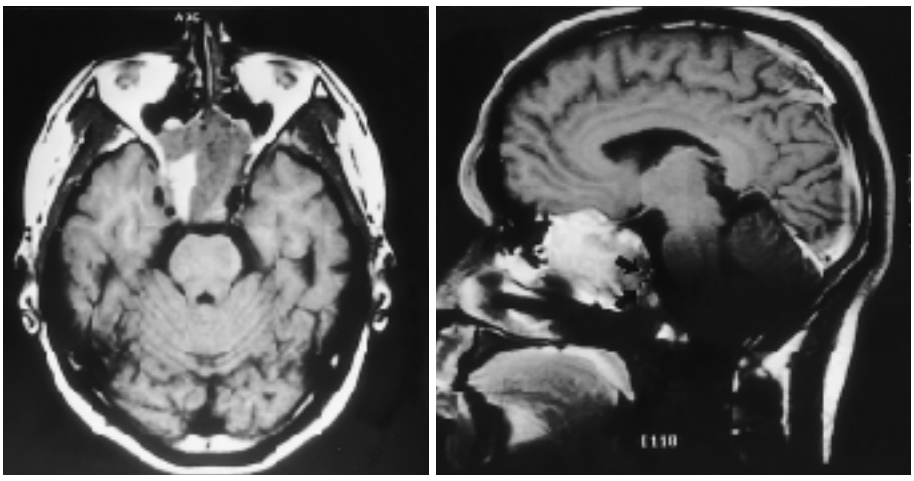

A B

Fig. 2. Cavernous sinus invasion of olfactory neuroblastoma in a 24-year-old man. Precontrast T1-weighted MR image (A) shows a hypointense tumor involving the ethmoid and sphenoid sinuses. On Gadolinium-enhanced T1-weighted sagittal MR image (B), the internal carotid artery (arrows) is encased by the mass. Note strong enhancement of the tumor.

scan of the area above the ethmoid sinus was not available. The evaluation of intracranial tumor extension seen on initial images was thus possible in 14 patients, and in nine of these (64 %), extension was demonstrated. Frank mass formation in the brain, with adjacent parenchymal edema, was demonstrated in four of these nine (44 %), and remaining five, discontinuity of the bony cribriform plate was definite, but only dural enhancement or thickening was present, with no evidence of intracranial tumor formation (Fig. 3). Follow up images showed intracranial tumor involvement in two further patients. Intracranial tumor extension was thus seen in a total of 11 patients (73 %). Three of nine masses with intracranial extension had intratumoral cystic areas in their intracranial portion (Fig. 4). Two masses had cysts in their peripheral margins, but in one case, the cystic area was in the center of the mass. In two cases, the interface between solid areas and cystic portions of the tumor was convex to the direction of cystic areas. In no patient cystic lesion was detected in the extracranial portion of the tumor.

Lymph node metastasis occurred in six of twelve patients; this involved the jugulodigastric chain in four, the retropharyngeal chain in two, and the posterior spinal accessory chain in two (Fig. 5). The mean diameter of primary tumor with lymph node metastasis was 6.2 cm, which was greater than that without regional lymph node metastasis (4.6 cm). Both patients with retropharyngeal node metastasis were less than twenty years old.

On MRI, eight of 12 masses showed low signal intensity on T1-weighted images, three masses showed iso-signal intensity and only one mass showed slightly higher signal intensity than gray matter. On T2-weighted images, the mass showed iso- or high signal intensity in 11 cases, and in only one patient was the signal intensity of the tumor lower than that of gray matter. In 11 patients, the tumor showed a prominent enhancement pattern on post-contrast enhanced images, and minimal tumor enhancement was seen in the other. CT scans also demonstrated prominent tumor enhancement in all 12 patients.

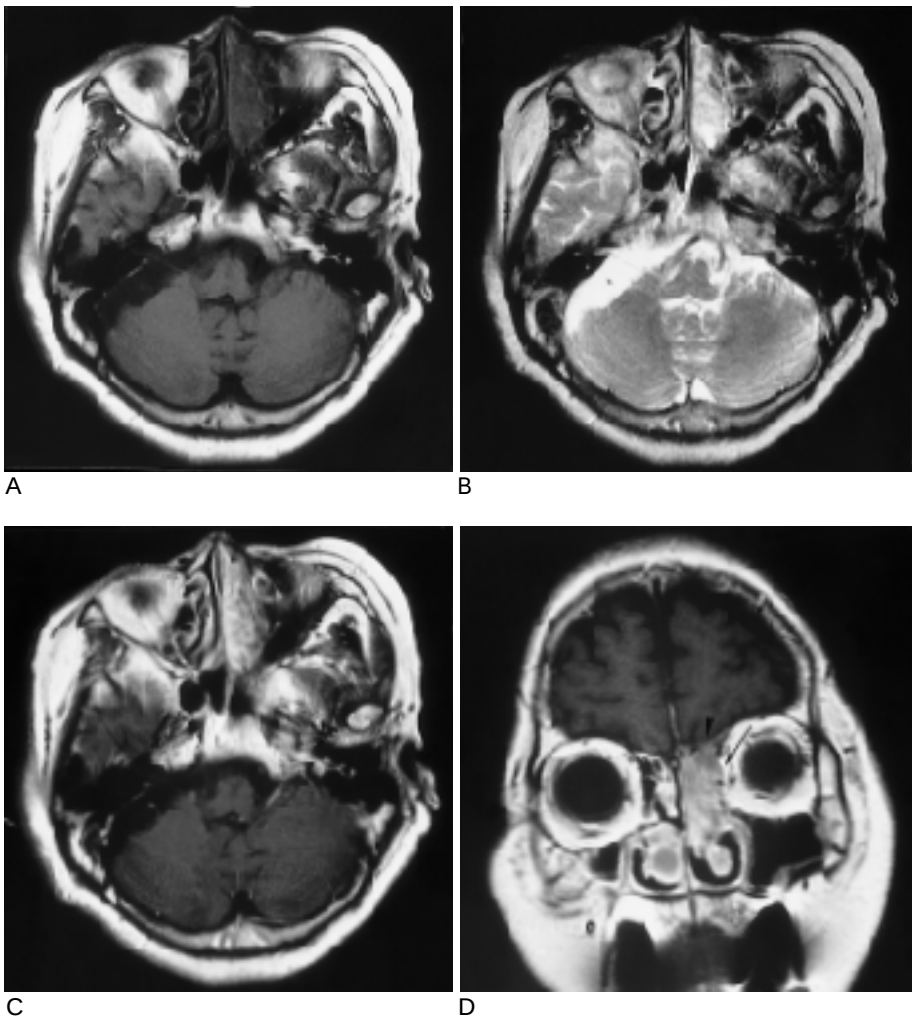

Fig. 3. Intracranial involvement of olfactory neuroblastoma in a 63-year-old female. Precontrast T1-weighted axial MR image (A) shows a hypointense tumor involving the left ethmoid sinuses and the left nasal cavity. On T2-weighted axial MR image (B), the tumor is seen as hyperintensity. Gadolinium-enhanced T1-weighted axial (C) and coronal (D) MR image shows intense enhancement of the tumor. Note the discontinuation of hypointense bony cortex in the cribriform plate (arrowhead) and medial wall of the left orbit (arrow).

Discussion

Olfactory neuroblastomas are unusual tumors that arise primarily in the nasal fossa and are considered to be one of the differential diagnoses of masses in the superior nasal vault. Normally, olfactory epithelium can exist in any area between the cribriform plate and the level of the middle turbinates, and olfactory neuroblastomas can therefore arise in that area with the same distribution as that of olfactory epithelium (11). Primary parasellar, nasopharyngeal, and paranasal sinus lesions

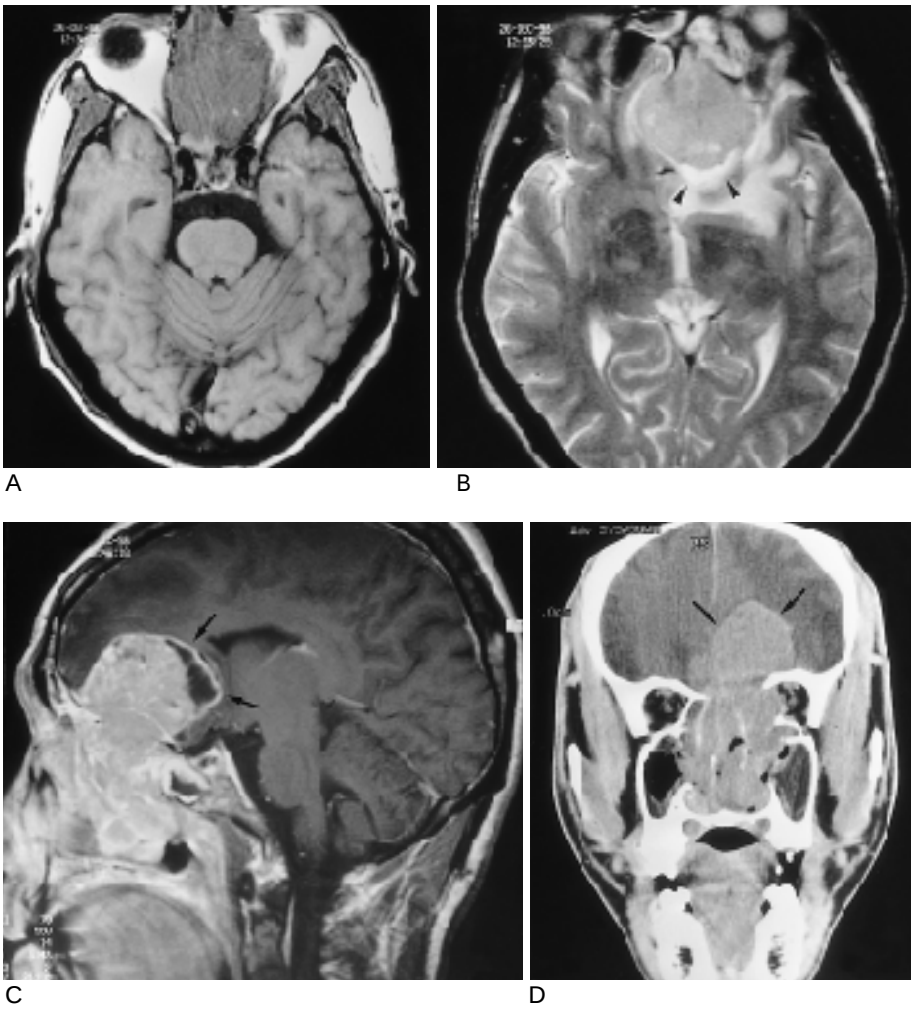

Fig. 4. Intracranial mass formation of olfactory neuroblastoma in a 42-year-old man. T1-weighted axial MR image (A) shows a mass involving the nasal cavity, ethmoid sinus, and the left orbit. T2-weighted axial MR image (B) at the upper level shows a hyperintense mass that extends contiguously from the sinonasal mass. There is a crescent-shaped area (arrowheads) in the periphery of the mass. It has the same signal intensity as that of CSF. On Gadolinium-enhanced T1-weighted sagittal MR image (C), the intratumoral cystic area has well-demarcated margin with prominent rim enhancement. Contrast enhanced coronal CT image (D) shows large intracranial tumor extension (arrows).

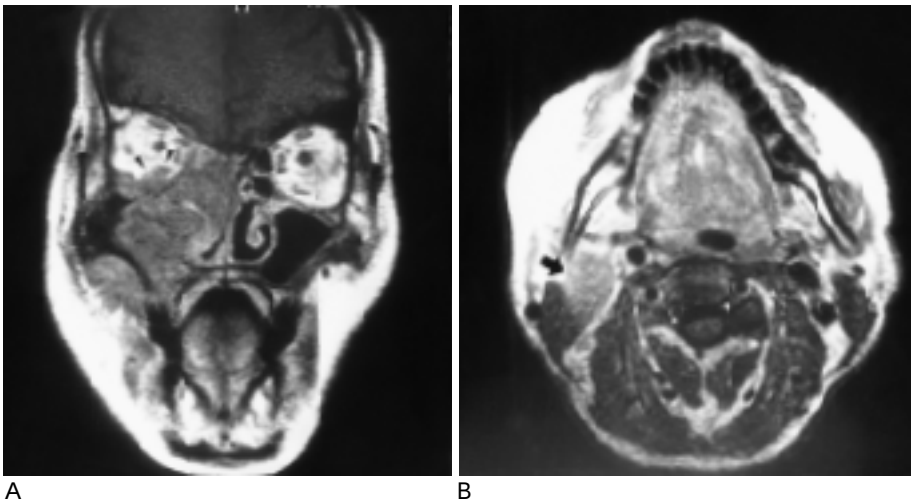

Fig. 5. Regional lymph node metastasis of olfactory neuroblastoma in 52-year-old man. Gadolinium-enhanced T1-weighted coronal MR image (A) shows a large tumor, involving the right nasal cavity, paranasal sinuses including the maxillary sinus, and the right orbit. Note the gross mass formation (arrowhead) in the right orbit. Gadolinium-enhanced T1-weighted axial MR image (B) shows an enlarged lymph node (arrow) in the right internal jugular chain.

have been described in the literature, though we have not encountered such cases (2, 12-14). In our series, the most common CT or MR imaging appearance of olfactory neuroblastomas at the time of initial diagnostic workup was a mass in the superior nasal cavity or ethmoid sinus, with destruction of the cribriform plate and involvement of the lateral nasal wall including the lamina papyracea.

Intracranial extension was common, although gross invasion and mass formation in the parenchyma of the brain were found in less than half of all cases with intracranial tumor extension. Kadish classified three groups for the staging of olfactory neuroblastoma: Group A, a tumor confined to the nasal cavity; Group B, a tumor involving the nasal cavity and paranasal sinuses; and Group C, a tumor which has spread beyond the nasal cavity and paranasal sinuses (15).

In our study, most but not all olfactory neuroblastomas invaded the cribriform plate or orbital wall, causing bony erosion or destruction, and most thus belonged to Kadish group B or C. This result may represent the uppermost location of a primary tumor in the nasal cavity, rather than an exclusive feature of the tumor itself. Any malignant tumors other than olfactory neuroblastomas originating from the superior nasal cavity or ethmoid sinus readily demonstrate invasion of adjacent structures such as the olfactory bulb, anterior cranial fossa, orbits, and paranasal sinuses (9, 16). Although olfactory neuroblastoma is a unilateral mass, our series showed that extension of the mass involved the opposite nasal cavity or paranasal sinuses.

Common sense suggests that the greater the diameter of the primary mass, the higher the likelihood that the tumor will invade adjacent structures, and our results support this supposition. In two cases in our series with intraorbital tumor extension, the tumor was smaller than average, and without intraorbital extension. Thus, a small primary mass does not necessarily imply confinement in nasal cavity, or that the tumor is at a lower stage.

Furthermore, tumor invasion of adjacent paranasal sinuses, especially the ethmoid sinus, was detected in all patients in our series. Kadish reported the percentage of stage A as about 40 % (15), but according to his staging, no patient in our series belonged to stage A; in most of our patients the tumor invaded the ethmoid sinuses. Other reported imaging studies have presented similar results (7, 17). One report dealing with the clinicopathological features of olfactory neuroblastoma showed that only one of 21 cases belonged to Group A (18). The significant discrepancy between Kadish 's results and those of other investigators may be due to the fact that his study did not include cross sectional images, and tumor imaging involved only roentgenological evaluation. Thus, in his study, the extent of primary tumor could be underestimated.

In olfactory neuroblastomas, the detection of intracranial tumor extension is very important in tumor staging and planning in relation to radiation ports or craniofacial surgery. In olfactory neuroblastomas, the reported rate of gross intracranial spread is about 30 % (15). In five patients, in our study with intracranial tumor extension, average mass size (6.4 cm) was greater than in those without such extension (4.5 cm). Due to the small sample size in our series, the significant difference in tumor size between these two groups is unknown. One patient with a 4.5cm-sized tumor showed intracranial extension, but the size in this case was the same as the average size of a tumor without intracranial extension. Thus, tumor growth to a certain critical size may not always precede intracranial extension of olfactory neuroblastoma.

MR generally fails to demonstrate a small area of bony destruction in the floor of the anterior cranial fossa, so the image is not as clear as those obtained by CT. More than a few millimeters of bony defect may, however, be detected on MR as an area of absent signal void in the bone. Pamela et al. suggested that the decreased sensitivity of MRI in detecting minimal bone erosion can be overcome by the use of Gd-DTPA, which shows abnormal enhancement at the site of bony defect and the enhancing epidural tumor bulge (19). We agree with the results of another report which claims that due to its unique capability of multiplanar imaging, MR is superior to CT both in distinguishing a tumor from associated inflammatory disease and in tumor mapping (11). On the other hand, because CT more clearly demonstrates bony structures, subtle erosion of the cribriform plate and roof of the ethmoid sinus is more easily demonstrated on CT than on MRI (20). In cases of contiguous tumor spread to adjacent structures, frank bony destruction is also detected more easily on CT, appearing as discontinuity of markedly high-attenuated bony structures by primary mass, with soft tissue attenuation.

In view of the fact that tumor staging is determined on the basis of invasion of adjacent anatomical compartments, and that MR is superior to CT in tumor mapping, CT demonstration of bony destruction does not seem to

provide radiologists with additional information about tumor staging, or offer clinicians a treatment plan. Our series showed that a tumor invariably involves the lamina papyracea, and that at the time of initial imaging there may also be frank bony destruction. The erosion of adjacent bony structures does not influence the staging of this neoplasm, and this is not a specific finding of nasal tumors. Where there is no detectable bony erosion of lamina papyracea in a case involving nasal mass imaging, this finding can, however, help exclude the diagnostic possibility of olfactory neuroblastoma.

In our series, three tumors of five with intracranial tumor extension had intratumoral cystic areas involving the brain, and one report insisted that such a finding should be one of the specific imaging characteristics of olfactory neuroblastoma (21). However, our study did not include sinonasal tumors other than olfactory neuroblastomas, and for confirmation of this finding as a valuable diagnostic feature, further studies must be undertaken.

Except in one case, our study did not reveal any cystic areas in the extracranial portion of the mass, as seen on cross- sectional images. There was no evident extracranial cystic or hemorrhagic area, even in masses in which the cystic portion lay within intracranial areas, as in two of three cases. Although histologic evaluation of olfactory neuroblastomas readily shows necrotic areas, other radiological reports reached the same conclusions as ours (19, 22). This result implies that intracranial cystic or hemorrhagic areas of this neoplasm might not represent specific biologic features of the tumor itself, but could be the products of unknown interaction between a tumor and the brain.

In cases of olfactory neuroblastoma, the establishment of a proper treatment plan depends on the evaluation of regional lymph nodes. According to many clinical studies of olfactory neuroblastoma, metastasis to cervical lymph nodes, the liver, bone and other sites occurs in 14-20 % of patients (15, 23, 24). In our series, the regional lymph node metastasis rate was 50 %, a higher percentage than that noted in other studies. The mean diameter of primary tumor with lymph node metastasis was larger than that in which there was no such metastasis. Due to the small sample size, the significance of these values is unknown, but the result shows an increased incidence of regional metastasis in advanced tumors. In general, metastasis of nasal mass occurs initially via the retropharyngeal chain, but repeated infection in childhood makes obliteration of lymph nodes in retropharyngeal areas. This fact could explain the absence, in our series, of lymph node metastasis in adult via the retropharyngeal chain.

The features of this tumor revealed by CT, namely that it is a homogeneous soft tissue mass showing uniform enhancement in the superior nasal cavity (25), were reconfirmed in our study. All the masses in our series showed a prominent enhancement pattern on CT scans. It is well known that the MR appearance of olfactory neuroblastoma is variable (7, 15, 19).

In conclusion, our study showed that olfactory neuroblastomas generally belong to Kadish stage B or C at the time at which symptoms are apparent. Intracranial tumor extension was frequent, but frank mass formation large enough to be detected radiologically was seen in less than half of all cases. Regional lymph node metastasis was also frequent.

References

1. Hyams VJ. *Olfactory neuroblastoma*. In: *Contemporary issues in surgical pathology, vol 10.* New York: Churchill Livingston, 1988; 483-488
2. Som PM, Shapiro MD, Biller F, Sasaki C, Lawson W. Sinonasal tumors and inflammatory tissues: differentiation with MR imaging. *Radiology* 1988;167:803-808
3. Yousem DM, Fellows DW, Kennedy DW, Bolger WE, Kashima H, Zinreich SJ. Inverted papilloma: evaluation with MR imaging. *Radiology* 1992;185:501-505
4. Micheau C. A new histochemical and biochemical approach to olfactory esthesioneuroblastoma. A nasal tumor of neural crest origin. *Cancer* 1977;40:314-318
5. Taxy J, Hidvegi DF. Olfactory neuroblastoma. An ultra-structural study. *Cancer* 1977;39:131-136
6. Chuadhy AP, Haar LG, Koul A, Nickerson PA. Olfactory neuroblastoma (esthesioneuroblastoma). A light and ultra-structural study of two cases. *Cancer* 1979;44:564-579
7. Derdeyn CP, Moran CJ, Chason DP, Koby MB, Rodriguez F. MRI of esthesioneuroblastoma. *J Comput Assist Tomogr* 1994; 18:16-21
8. Burke DP, Gabrielsen TO, Knake JE, Seeger JF, Oberman HA. Radiology of olfactory neuroblastoma. *Radiology* 1990;137:367-372
9. Som PM., Brandwein M. *Sinonasal cavities: inflammatory disease, tumors, fractures, and postoperative findings.* In Som PM, Curtin HD, eds. *Head and neck imaging.* 3rd ed. St. Louis : Mosby, 1996; 126-315
10. Schuster JJ, Phillips CD, Levine PA. MR of esthesioneuroblastoma (olfactory neuroblastoma) and appearance after craniofacial resection. *AJNR Am J Neuroradiol* 1994;15:1169-1177
11. Shah JP, Feghali J. Esthesioneuroblastoma CA 1983; 33:154-159
12. Sarwar M. Primary sellar-parasellar esthesioneuroblastoma. *AJR* 1979;133:140-141
13. Rogengren JE, Jing B, Wallace S, Danziger J. Radiographic features of olfactory neuroblastoma. *AJR* 1979;132:945-948
14. Jansen KJ, Elbrune O, Lund C. Olfactory esthesioneuroblastoma. *J Laryngol Otol* 1976;90:1007-1013
15. Kadish S, Goodman M, Wine CC. Olfactory neuroblastoma: a clinical analysis of 17 cases. *Cancer* 1976;37:1571-1576

16. Barnes L, Peel RL, Verbin SR. *Tumors of the nerves system*. In: Bernes L, ed. *Surgical pathology of the Head and neck*. Vol 1. New York: Marcel Decker, 1985;675-724
17. Li C, Yousem DM, Hayden RE, Doty RL. Olfactory neuroblastoma: MR evaluation. *Radiographics* 1996;16:1101-1110
18. Mills SE, Frierson HF. Olfactory neuroblastoma. *AJNR Am J Neuroradiol* 1993; 14:1167-1171
19. Pamela VT, Ya-Yen L. Gd-DTPA enhanced MR for detecting intracranial extension of sinonasal Malignancies. *J Comput Assist Tomogr* 1991;15:387-392
20. Paling MR, Black WC, Levine PA, Cantrell RW. Tumor invasion of the anterior skull base: a comparison of the MR and CT studies. *J Comput Assist Tomogr* 1987;11:824-830
21. Som PM, Brandwein M, Catalano P, Biller HF. Sinonasal esthesioneuroblastoma with intracranial extension: marginal tumor cysts as a diagnostic MR finding. *AJNR Am J Neuroradiol* 1994;15: 1259-1262
22. Manelfe C, Bonalfe A, Fabre P, Pessey JJ. Computed tomography in olfactory neuroblastoma: One case of esthesioneuroepithelioma and four cases of esthesioneuroblastoma. *J Comput Assist Tomogr* 1978;2:412-420
23. Homzie MJ, Elkon AD. Olfactory esthesioneuroblastoma: variable prediction of tumor control and recurrence. *Cancer* 1980;46:2509-2513
24. Spauldingn CA, Kronyak MS, Constable WC, Stewart FM. Esthesioneuroblastoma: a comparison of two treatment era. *Int J Radiat Oncol Biol Phys* 1988;15:581-590
25. Hurst RW, Erickson S, Cail WS, et al. Computed tomographic features of esthesioneuroblastoma. *Neuroradiology* 1989;31:253-257

대한방사선의학회지 2000;42:417-424

후각 신경아세포종: CT와 MR 소견[1]

[1]서울대학교 의과대학 방사선과학교실, 서울대학교 의학연구원 방사선의학연구소

이동경 · 한문희 · 김홍대 · 장기현 · 강흥식 · 연경모

목적 : 후각 신경아세포종의 전산화 단층 촬영(CT)와 자기공명 영상(MRI) 소견을 알아보고자 하였다.
대상과 방법 : 병리학적으로 후각 신경아세포종으로 확진 된 15명의 환자를 대상으로 하였다. CT를 12명의 환자에서 시행했고 MR을 11명에서 시행했다. 각 영상에서 종양의 파급 범위와 진단 당시의 크기, 조영 증강 양상, 종양에 의한 골조직 미란이나 파괴, 두경부의 림프절종대, 종양 내 낭성 영역의 존재의 유무 등을 분석하였다.
결과 : 종양은 모든 환자에서 상비강이나 사골동에 중심을 두고 있었으며 내측 안와벽을 포함한 비강의 침범이 14명의 환자에서, 사상형 평판의 침범이 13명에서 관찰되었다. 두개내 종양 침범이 9명에서 보였으나 두개내 종괴형성은 4명에서만 관찰되었다. 종양은 MR에서는 T1 강조영상에서12명 중 8명에서 고 신호강도를 나타내었고, T2 강조영상에서는 11명에서 중등도 이상의 신호강도를 보였으며 11명에서 조영 증강이 잘 되었다. CT에서는 11명 모두에서 종양의 조영 증강이 뚜렷하게 보였다. 림프절 종대는 12명 중 6명에서 관찰되었다.
결론 : 후각 신경아세포종은 대부분 영상 진단 당시 부비동과 안와를 침범하여 Kadish B 또는 C 시기에 해당된다. 종양의 두개내 침범은 흔하나 영상 진단에서 발견될 정도로 정도의 두개내 종괴를 형성하는 경우은 전체 두개내 침범의 절반 이하를 차지하며 국소적 림프절 전이도 흔하다.